Laboratory Investigation
https://doi.org/10.1038/s41374-018-0029-4

ARTICLE

NLRP3 inflammasome inhibition ameliorates tubulointerstitial injury in the remnant kidney model

Orestes Foresto-Neto[1] · Victor Ferreira Ávila[1] · Simone Costa Alarcon Arias[1] · Fernanda Florencia Fregnan Zambom[1] · Lisienny Campoli Tono Rempel[1] · Viviane Dias Faustino[1] · Flavia Gomes Machado[1] · Denise Maria Avancini Costa Malheiros[1] · Hugo Abensur[1] · Niels Olsen Saraiva Camara[1,2] · Roberto Zatz[1] · Clarice Kazue Fujihara[1]

Received: 29 September 2017 / Revised: 6 December 2017 / Accepted: 2 January 2018

Abstract

Recent studies suggest that NLRP3 inflammasome activation is involved in the pathogenesis of chronic kidney disease (CKD). Allopurinol (ALLO) inhibits xanthine oxidase (XOD) activity, and, consequently, reduces the production of uric acid (UA) and reactive oxygen species (ROS), both of which can activate the NLRP3 pathway. Thus, ALLO can contribute to slow the progression of CKD. We investigated whether inhibition of XOD by ALLO reduces NLRP3 activation and renal injury in the 5/6 renal ablation (Nx) model. Adult male Munich–Wistar rats underwent Nx and were subdivided into the following two groups: Nx, receiving vehicle only, and Nx + ALLO, Nx rats given ALLO, 36 mg/Kg/day in drinking water. Rats undergoing sham operation were studied as controls (C). Sixty days after surgery, Nx rats exhibited marked albuminuria, creatinine retention, and hypertension, as well as glomerulosclerosis, tubular injury, and cortical interstitial expansion/inflammation/fibrosis. Such changes were accompanied by increased XOD activity and UA renal levels, associated with augmented heme oxigenase-1 and reduced superoxide dismutase-2 renal contents. Both the NF-κB and NLRP3 signaling pathways were activated in Nx. ALLO normalized both XOD activity and the parameters of oxidative stress. ALLO also attenuated hypertension and promoted selective tubulointerstitial protection, reducing urinary NGAL and cortical interstitial injury/inflammation. ALLO reduced renal NLRP3 activation, without interfering with the NF-κB pathway. These observations indicate that the tubulointerstitial antiinflammatory and antifibrotic effects of ALLO in the Nx model involve inhibition of the NLRP3 pathway, and reinforce the view that ALLO can contribute to arrest or slow the progression of CKD.

Introduction

Chronic kidney disease (CKD) is a worldwide health problem with high rates of mortality and need for renal replacement therapy. Early intervention against risk factors involved in the pathogenesis of CKD is crucial to avoid the progression of the disease. CKD is characterized by progressive proteinuria, hypertension, chronic inflammation and oxidative stress that lead to loss of renal function and fibrosis. Recently we showed that renal inflammasome activation occurs as early as fifteen days after 5/6 renal ablation (Nx), and persists through advanced phases of this CKD model [1]. Additional recent observations suggest that renal inflammasome is activated in patients with CKD and in animal models of this condition [2−5], and that its deficiency prevents kidney injury [6].

The Nucleotide-binding oligomerization domain, Leucine-rich Repeat and Pyrin domain containing-3 (NLRP3) belongs to the NLR family of pattern recognition receptors. It forms a complex with Apoptosis-associated Speck-like protein containing a Caspase recruitment domain adaptor protein (ASC), and the caspase 1 protease to generate a multiprotein inflammasome complex,

✉ Orestes Foresto-Neto
forestoneto@usp.br

✉ Roberto Zatz
roberto.zatz@gmail.com

[1] Renal Division, Department of Clinical Medicine, Faculty of Medicine, University of São Paulo, São Paulo, Brazil

[2] Laboratory of Transplantation Immunobiology, Institute of Biomedical Sciences, University of São Paulo, São Paulo, Brazil

Published online: 06 March 2018

which, upon activation, catalyzes the conversion of pro-interleukin-1β and -18 into their mature forms [7, 8], thus promoting tissue influx of leukocytes and favoring inflammation.

Activation of the NLRP3 inflammasome complex is triggered by recognition of cellular damage-associated molecular patterns (DAMPs) and pathogen-associated molecular patterns (PAMPs). A diversity of DAMPs is capable of activating the NLRP3 inflammasome, e.g. reactive oxygen species (ROS), nucleic acids, extracellular ATP, and uric acid (UA) [9–13].

The role of UA in the pathogenesis of CKD has yet to be clarified. It was once thought that, to cause renal inflammation and CKD, UA had to crystallize, just as in joints of gout patients. However, recent studies indicated that soluble UA can also activate the NLRP3 inflammasome in renal tissue [13, 14]. It is unclear to what extent this process is favored by UA itself, as xanthine oxidase (XOD) catalyzes the transformation of hypoxanthine into xanthine, as well as xanthine oxidation to UA. In this process, ROS are also generated, which may also activate the NLRP3 inflammasome [15].

XOD activity can be inhibited by allopurinol (ALLO), which has a double-tracked beneficial effect: on one hand, ALLO reduces the levels of UA [16]. On the other, by diminishing ROS production, ALLO exerts antioxidant and antiinflammatory effects [17, 18], which may also contribute to prevent renal injury [19, 20].

Patients with CKD and high UA levels are frequently treated with ALLO in order to avoid complications such as gout. However whether ALLO treatment exerts a protective effect against progression of CKD has not been unequivocally determined [21]. In the present study, we investigated the hypothesis that inhibition of XOD by ALLO prevents NLRP3 inflammasome activation and slows the progression of CKD.

Materials and Methods

Experimental protocol

Eighty-two adult male Munich–Wistar rats, weighing 230–250 g, were used in this study. The rats were obtained from a local facility at the Faculty of Medicine, University of Sao Paulo. The experimental procedures were specifically approved by the local Research Ethics Committee (CAPPesq, process no. 456/11) and developed in strict conformity with our institutional guidelines and with international standards for the manipulation and care of laboratory animals. Five-sixths renal ablation (Nx) was performed in a single-step procedure. After ventral laparotomy, rats were anesthetized with ketamine (50 mg/kg im) and xylazine (10 mg/kg im), the right kidney was removed, and two or three branches of the left renal artery were ligated, resulting in the infarction of two-thirds of the left kidney. Sham-operated rats, used as controls, underwent anesthesia and manipulation of the renal pedicles without any reduction of renal mass. After surgery, all animals received a single dose of enrofloxacin (5 mg/kg im) and tramadol hydrochloride (10 mg/kg) and, after full recovery, were given free access to tap water, fed regular rodent chow containing 0.5 Na and 22% protein (Nuvital Labs, Curitiba, Brazil), and kept at 23 ± 1 °C and 60 ± 5% relative air humidity under an artificial 12:12-h light–dark cycle. Allopurinol (ALLO) treatment (36 mg/kg per day in the drinking water) was started on the day after renal ablation. Nx rats were randomized into two groups: untreated Nx rats (Nx group; $n = 28$), Nx rats that received ALLO as described earlier (Nx + Allo group; $n = 29$). Sham-operated rats (C group; $n = 25$) received no treatment. All groups were followed for 60 days. At the end of the study, tail-cuff pressure (TCP) was determined with an optoelectronic automated device (BP 2000 Blood Pressure Analysis System, Visitech Systems, EUA) after rats had been preconditioned to the procedure [22], and urinary albumin excretion (ALB) was assessed by radial immunodiffusion. The animals were then anesthetized as described above. Blood samples were taken from the abdominal aorta for biochemical analyses, and left kidney was retrogradely perfused in situ through the abdominal aorta with saline to remove blood from renal vessels. In 10–11 animals of each group, the remnant kidney (left kidney in the Control Group) was perfusion-fixed with Dubosq-Brazil solution. Subsequently, two midcoronal kidney slices were postfixed in buffered 10% formaldehyde solution, and embedded in paraffin using conventional sequential techniques. Histomorphometric and immunohistochemical analyses of the renal tissue were performed in 4-mm-thick sections. In 15–18 animals of each group, the left kidney was perfused with saline only, excised and rapidly frozen at −80 °C for protein assessment or isolation of nuclei. For the ELISA and western blot analyses, we used ten animals per group. The histomorphometric and immunohistochemical analyses were performed in eight animals per group. The remaining parameters were determined in all animals of each group.

Biochemical and enzymatic analyses

Serum creatinine (SCr) was determined using a commercially available kit (Labtest Diagnostica, São Paulo, Brazil). The renal XOD activity was quantified using a fluorometric assay kit (Cayman, Michigan, USA) and the renal UA content was measured in kidney homogenates, using a commercial kit (Labtest Diagnostica, São Paulo, Brazil).

Histomorphometric analysis

For assessment of the glomerular injury, 4-μm-thick sections were stained by the periodic acid-Schiff reaction. The extent of glomerular damage was estimated by determining the frequency of glomeruli with sclerotic lesions (GS), as described previously [23]. Masson's trichrome was used to measure the percentage of renal cortical area (INT), which was estimated by a point-counting technique.

Immunohistochemical analysis

Immunohistochemical analyses were performed on 4-μm-thick renal sections mounted on 2% silane coated glass slides. The following primary antibodies were employed: monoclonal mouse anti-rat ED-1 (Serotec, Oxford, UK) for macrophages; polyclonal rabbit anti-collagen I (Abcam, Cambridge, UK); polyclonal rabbit anti-NLRP3 (Sigma, Saint Louis, USA). Details of the techniques for ED-1 and type-I collagen immunohistochemistry are given elsewhere [22]. For NLRP3 detection, sections were pretreated with 30% hydrogen peroxide in methanol and preincubated with serum-free protein block (Dako, Glostrup, Denmark). The primary antibody was diluted at 1:400 in 1% bovine serum albumin (BSA). After rinsing with tris-buffered saline (TBS), sections were incubated with HRP-labeled polymer conjugated with secondary antibodies (Dako, Glostrup, Denmark), then with DAB substrate-chromogen solution (Dako, Glostrup, Denmark) for development. The renal density of ED-1-positive cells was evaluated in a blinded manner at ×400 magnification. The percentage of cortical interstitial area occupied by collagen I and the percentage of glomerular area staining positively for NLRP3 were estimated by the same point-counting technique employed to evaluate INT, under ×400 magnification. For the estimation of cortical interstitial NLRP3, the number of cells per mm^2 was evaluated under ×400 magnification. For each section, 50 microscopic fields (corresponding to a total area of 1.6 mm^2) were examined.

Total protein isolation and isolation of nuclei

Renal proteins were extracted using lysis buffer (Thermo Scientific, Rockford, USA) with protease and phosphatase inhibitor (Roche, Mannheim, Germany). Protein concentration was determined with the bicinchoninic acid (BCA) method. For isolation of nuclei, kidney tissues were homogenized on ice with special glass pestle (Sigma Aldrich, Saint Louis, USA) in lysis buffer and centrifuged at $1000 \times g$ for 10 min at 4 °C to obtain a crude nuclear pellet. The supernatant (cytosolic fraction) was discarded. Further the pellet was reconstituted in high sucrose Laemmli buffer and centrifuged at $1500 \times g$ for 10 min at 4 °C to obtain a pure nuclear suspension.

Western blot assays

For western blot analysis, 100 μg of total proteins were mixed with 2× Laemmli loading buffer and were denatured at 96 °C for 5 min. For the specific nuclear fraction analysis, the preconditioned samples were not denatured. Protein separation was performed by sodium dodecyl sulphate-polyacrylamide gel electrophoresis. The separated proteins were transferred to a nitrocellulose membrane. The membrane was incubated with 5% non-fat milk or 5% BSA in TBS for 1 h at room temperature to block nonspecific binding. The membrane was then incubated overnight at 4 °C with primary antibodies for: β-actin, 1:5000 (Sigma Aldrich, Saint Louis, USA); caspase 1, 1:1000 (Santa Cruz Biotechnology, Santa Cruz, USA); heme oxygenase 1 (HO-1), 1:500 (Abcam, Cambridge, UK); superoxide dismutase 2 (SOD2), 1:10000 (Cayman, Michigan, USA); phosphorylated nuclear factor kappa B (NF-κB) p65 component, 1:100 (Cell Signaling Danvers, USA); histone H2B, 1:1500 (Abcam, Cambridge, UK). After rinsing with tris-buffered saline Tween 20 buffer (TBST), membranes were incubated with secondary antibodies labeled with HRP. Immunostained bands were detected using a chemiluminescence kit (Thermo Scientific, Rockford, USA), and were further analyzed by densitometry with a gel documentation system and the Uvisoft-UvibandMax software (Uvitec Cambridge, Cambridge, UK).

ELISA assays

Protein levels of NGAL, MCP-1, IL-1β and IL-10 were measured by ELISA. The concentration of NGAL was determined in the urine, using a rat NGAL ELISA kit (BioPorto, Copenhagen, Denmark). Total IL-1β and IL-10 were measured in homogenized kidney tissue. The serum concentration and the tissue content of MCP-1 were measured using a commercial kit (R&D Systems, Minneapolis, USA). All analyses were performed in accordance with the manufacturer's instructions.

Statistical analysis

Results are expressed as means ± SEM. Statistical differences among groups were assessed by one-way ANOVA (with Newman–Keuls post-test) [24]. Correlations were determined by calculating the Pearson's coefficient. Differences were considered significant at $P < 0.05$. All calculations were performed using GraphPad Prism 4.0 software.

Table 1 Body weight, albuminuria, serum creatinine and tail-cuff pressure 60 days after renal ablation

	C	Nx	Nx + ALLO
BW, g	309 ± 8	253 ± 6[a]	264 ± 6[a]
ALB, mg/24 h	3 ± 1	100 ± 14[a]	87 ± 16[a]
SCr, mg/dL	0.6 ± 0.1	1.2 ± 0.1[a]	1.1 ± 0.1[a]
TCP, mm Hg	134 ± 2	212 ± 8[a]	191 ± 6[ab]

Body weight (BW, g), urinary albumin excretion (ALB, mg/24 h), serum creatinine (SCr, mg/dL) and tail-cuff pressure (TCP, mm Hg) in C, Nx and Nx + ALLO groups. Results expressed as means ± SE

[a] $p < 0.05$ vs. C

[b] $p < 0.05$ vs. Nx

Results

Allopurinol reduced hypertension and attenuated tubulointerstitial injury

To address whether ALLO treatment exerts renoprotective effects on 5/6 renal ablation model (Nx), we evaluated physiologic and morphologic parameters after 60 days of treatment. Body weight (BW), albuminuria (ALB) and serum creatinine concentration (SCr) in Nx were not changed by ALLO. However, ALLO prevented the increase in tail-cuff pressure (TCP) (Table 1). We observed no difference between Nx and Nx + ALLO regarding glomerulosclerosis (GS) (Fig. 1a, d). Likewise, a significant increase of the fractional cortical interstitial area (INT) and an increased excretion of NGAL in the urine were observed in Nx, whereas ALLO was effective in preventing all these changes (Fig. 1b–c). Thus, ALLO had a protective effect on the tubule and interstitium in Nx, but no effect on glomerular damage.

Allopurinol attenuated renal inflammation and fibrosis

CKD is associated with a progressive increase in renal inflammation, and ALLO has been proposed as an antiinflammatory drug [18]. ALLO decreased serum and renal monocyte chemoattractant protein-1 (MCP-1) concentration, and suppressed renal interstitial macrophage infiltration in Nx animals (Fig. 2a–c, e). To understand the effect of ALLO on renal fibrosis, we analyzed the percentage of interstitial renal type 1 collagen expression. ALLO significantly suppressed the increased type 1 collagen staining observed in Nx (Fig. 2d–e). Thus, ALLO reduced the interstitial macrophage infiltration and fibrosis in the Nx model.

Xanthine oxidase inhibition by allopurinol resulted in lower uric acid levels and less oxidative stress

Renal XOD activity was significantly higher in Nx than in C rats. The XOD activity in Nx + ALLO was comparable to the observed in normal rats (Fig. 3a). Unlike humans, rats possess uricase, which promotes oxidative degradation of UA [25]. Despite the presence of uricase, UA levels were increased in Nx rats. Since uricase is mostly found in liver and kidneys of rats [26], the increased UA levels found in Nx could merely reflect the loss of renal mass. XOD activity inhibition with ALLO normalized renal UA in Nx (Fig. 3b). We then analyzed the oxidative stress resulting from increased XOD activity. HO-1 is an inducible enzyme with potent antioxidant action, which is increased in renal diseases as an adaptation to protect the kidney from ROS production [27]. SOD2, also known as manganese-dependent superoxide dismutase, transforms superoxide coming from mitochondrial electron transport chain into hydrogen peroxide, also protecting the cells from oxidative stress [28]. HO-1 content was increased, while the SOD2 expression was decreased, in Nx compared to C. ALLO reestablished the content of both enzymes, suggesting that oxidative stress was suppressed by treatment (Fig. 3c–e).

Allopurinol treatment reduced NLRP3 inflammasome activation

The NLRP3 inflammasome has been shown to play a role in the pathogenesis of CKD [2, 3]. We assessed the expression of components of the NLRP3 inflammasome complex in our model. Activated caspase 1 content was increased in Nx kidney compared to C, whereas ALLO reduced this parameter (Fig. 4a, b). NLRP3-positive staining was increased in both glomerular and tubulointerstitial areas in untreated Nx. Although ALLO treatment promoted no change in the glomerular NLRP3 content (Fig. 4c, i), it reduced the amount of NLRP3-positive cells in the tubulointerstitial compartment (Fig. 4d, i). Since the renal content of NLRP3 inflammasome components was increased in Nx, we investigated the renal abundance of IL-1β, which is the final product of this pathway [7, 8]. The IL-1β protein levels were increased in Nx, whereas ALLO reduced this parameter (Fig. 4e). The NF-κB system, when activated, promotes the transcription of genes related to proinflammatory proteins such as mcp-1, pro-il-1β and pro-il-18 [29]. Interestingly, NF-κB was activated in Nx, but ALLO did not interfere with this parameter (Fig. 4g, h). Further, we evaluated the ratio of the antiinflammatory IL-10 protein levels to the proinflammatory IL-1β. The IL-10/IL-1β ratio was diminished in Nx, whereas ALLO normalized this ratio (Fig. 4f). We concluded that ALLO inhibits the NLRP3 inflammasome activation, with reduction of the IL-1β production and increased antiinflammatory IL-10 levels. To investigate whether the effects of ALLO are mediated by NLRP3 activation, we performed correlation analyses. We observed that NLRP3 activation correlated positively with the density of macrophage infiltration (Fig. 5a) and with the

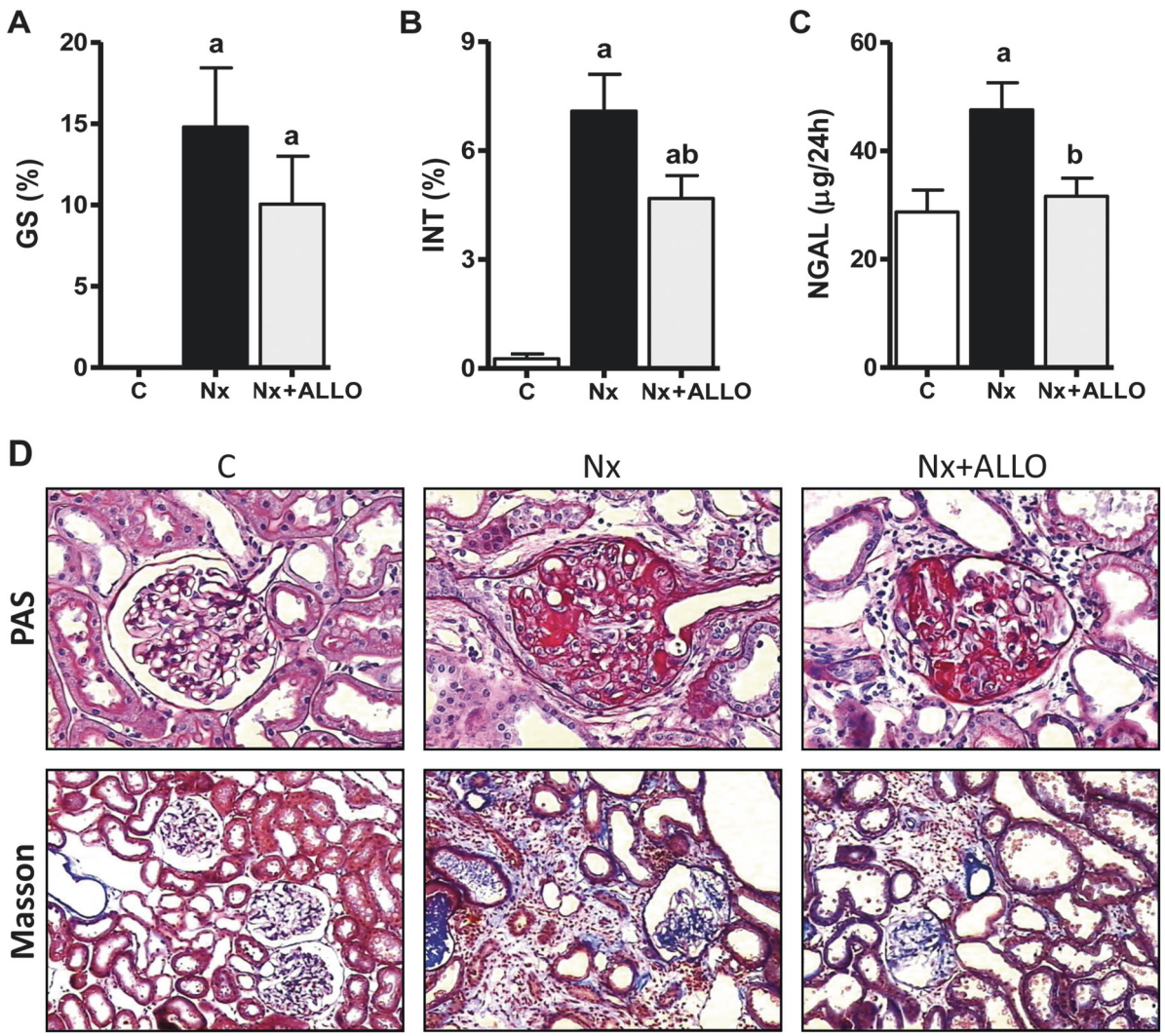

Fig. 1 Frequency of glomeruli with sclerotic lesions (GS, %) (**a**), percentage of cortical interstitial area (INT, %) (**b**), and urinary excretion of neutrophil gelatinase-associated lipocalin (NGAL, µg/24 h) in urine (**c**) 60 days after renal ablation. Periodic Acid-Schiff (PAS) (×400) staining was used to analyze glomerular injury, and Masson's trichrome (×200) was employed to evaluate the percentage of renal cortical interstitial area (**d**). Results expressed as means ± SE. $^{a}p < 0.05$ vs. C, $^{b}p < 0.05$ vs. Nx

percent cortical interstitial area (Fig. 5b) in Nx + ALLO. In addition, TCP correlated positively with the amount of NLRP3-positive cells (Fig. 5c) and with the renal IL-1β content (Fig. 5d) in Nx + ALLO, in consistency with the observed positive correlation between NLRP3 inhibition and parameters of renal injury in ALLO-treated rats. Together, the correlation data suggest that the protective effect of ALLO is associated with NLRP3 inhibition.

Discussion

As expected [30–34], renal ablation was accompanied by growth stunting, severe albuminuria, systemic hypertension, impaired renal function, renal inflammation, glomerulosclerosis and tubulointerstitial injury. The mechanisms involved in the progression of renal damage in this model are not yet fully understood, although it is well known that a number of inflammatory and hemodynamic factors can promote the progressive loss of nephrons, eventuating in the replacement of renal parenchyma by a fibrotic tissue.

We showed previously that the innate immunity and proinflammatory signaling pathway, NF-κB, is activated in the remnant kidney [35], and that its inhibition with pyrrolidine dithiocarbamate exerted a renoprotective effect [35]. Activation of this system leads to the transcription of a number of genes that codify for inflammatory mediators [29]. In the present study, we confirmed that the NF-κB system is activated in Nx rats, which may have contributed to enhance the expression of MCP-1 and IL-1β. The NLRP3 inflammasome is another innate immunity pathway activated in CKD [2, 3]. Recently, we showed that the renal

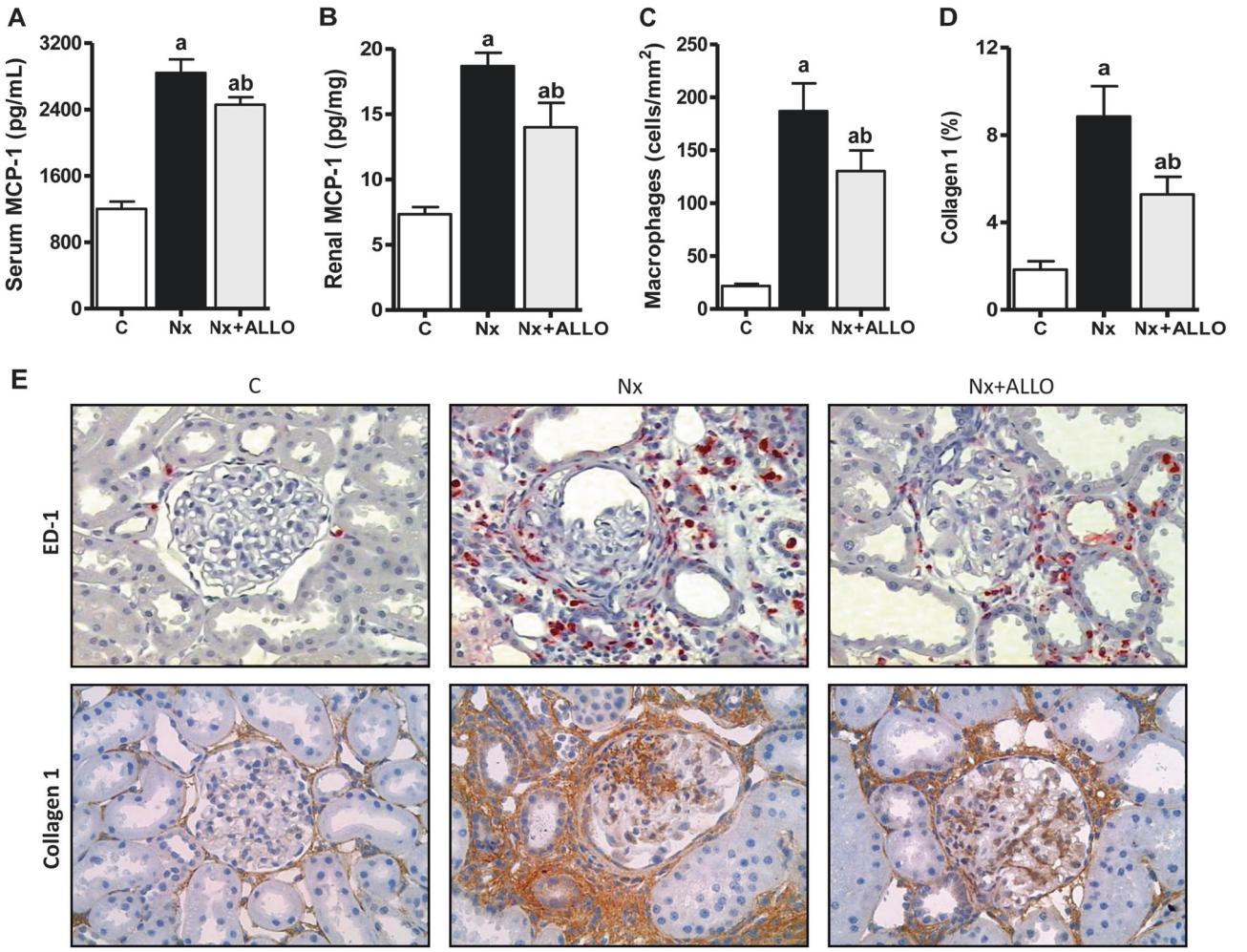

Fig. 2 Serum (**a**) and renal (**b**) content of monocyte chemoattractant protein-1 (MCP-1, pg/mL), interstitial macrophage infiltration (cells/mm^2) (**c**), and cortical interstitial area occupied by type-I collagen (%) (**d**). Immunohistochemistry was performed to identify and quantify macrophages (ED-1), stained in red, and collagen 1, stained in dark-brown (×400) (**e**). Results expressed as means ± SE. $^{a}p < 0.05$ vs. C, $^{b}p < 0.05$ vs. Nx

expression of NLRP3 is increased 15, 60 and 120 days after renal ablation [1]. Accordingly, we showed in the present study that the renal content of NLRP3 and mature caspase 1 was elevated 60 days after Nx, in association with increased IL-1β protein content, which exerts a proinflammatory effect in the renal tissue, promoting enhanced cytokine production and macrophage recruitment. Thus, activation of one or more innate immunity pathways was evident in Nx rats. The consequent trend toward renal inflammation in Nx rats was intensified by the observed downregulation of the antiinflammatory protein IL-10 in the remnant kidney.

The mechanisms by which innate immunity is activated in the Nx model and in other instances of CKD have not been determined. UA is one possible candidate. In the last few years, evidence that elevated UA levels can activate NLRP3 and cause renal damage has emerged [3, 4, 12]. In the present study, the renal UA content was moderately increased after 60 days of Nx, as a possible result of enhanced renal XOD activity. In addition to promoting UA production, XOD activation also results in ROS production, thus activating both the NF-κB and NLRP3 pathways [9, 36]. We showed HO-1 induction in the Nx group, suggesting an adaptation against the oxidative stress and other cytotoxic effects such as apoptotic cell death. In consistency with these results, SOD2, which promotes the conversion of O_2^- to H_2O_2 and O_2 [37], was diminished in Nx animals, suggesting a deficiency in the ROS removal after renal ablation, further contributing to oxidative stress.

ALLO prevented renal XOD activation and reduced hypertension, tubular injury (as shown by enhanced urinary NGAL), interstitial macrophage infiltration and interstitial fibrosis after 60 days of treatment. These data corroborate previous observations that ALLO exerts a considerable renoprotective and antiinflammatory effect [20]. However, ALLO treatment promoted no significantly reduction in

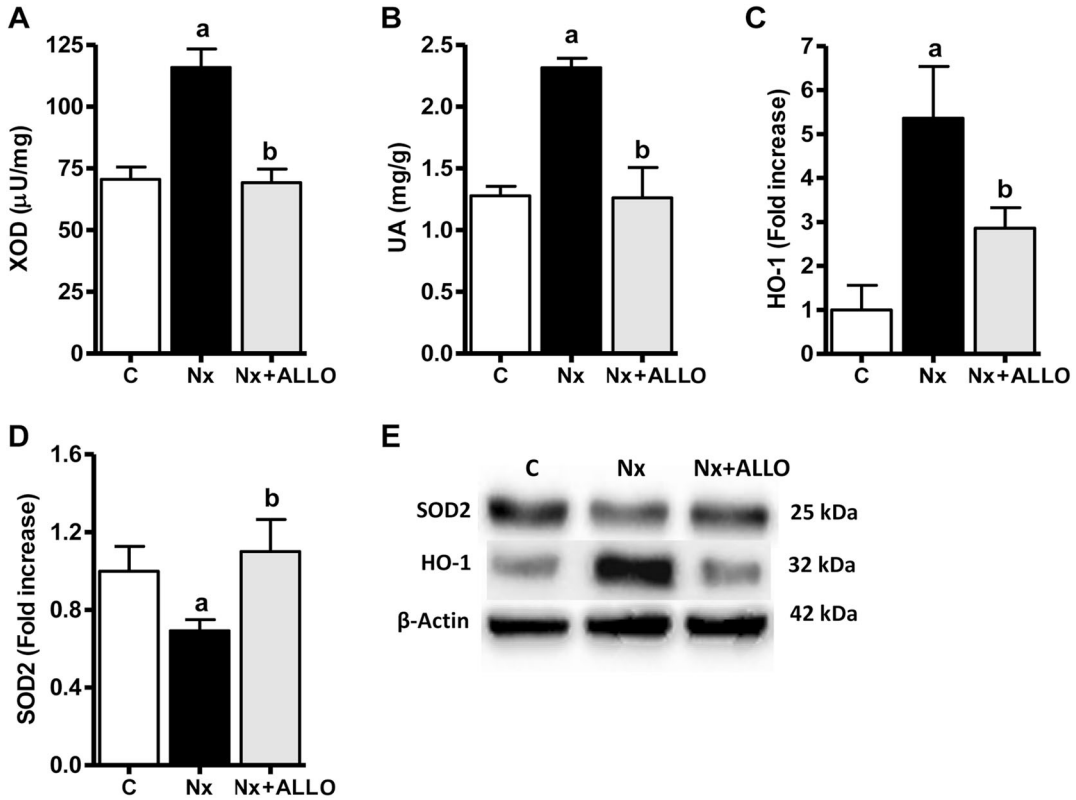

Fig. 3 Xanthine oxidase activity (XOD, µU/mg) (**a**) and uric acid concentration (UA, mg/g) (**b**) were evaluated in renal tissue using enzymatic assays. The renal contents of heme oxygenase 1 (HO-1) (**c**) and superoxide dismutase 2 (SOD2) (**d**) were quantified using western blot analysis (**e**). Results expressed as means ± SE. $^{a}p < 0.05$ vs. C, $^{b}p < 0.05$ vs. Nx

albuminuria or glomerular injury, indicating that renoprotection was confined to the interstitial compartment. This observation is consistent with previous clinical observations that ALLO may exert renoprotection without reducing proteinuria [16, 19]. In another study of the Nx model, ALLO reduced renal injury and proteinuria [38]. However, that study utilized rats made hyperuricemic by oxonic acid, and thus may not be comparable to our study.

Although the beneficial effect of reducing UA levels is self-evident in conditions such as gout, the mechanisms of ALLO renoprotection in CKD remain unclear. In the Nx model, Sanchez-Lozada et al. [38] showed that treatment with ALLO prevented glomerular hypertension in association with less inflammation. To date, a few clinical trials have assessed the potential role of reducing serum UA levels in the control of hypertension [39, 40]. In our study ALLO reduced UA in Nx as consequence of the XOD inhibition. However, it is well known that XOD inhibition by ALLO also reduces the synthesis of ROS [41]. Therefore, renoprotection by ALLO may have been at least in part independent of its action on renal UA content. Oxidative stress contributes to atherosclerosis, endothelial dysfunction and renal artery stenosis, all of which can lead to systemic hypertension [41, 42]. Nakazono et al. [43] demonstrated a causal link between oxidative stress and hypertension in spontaneously hypertensive rats, whereas treatment with ALLO reduced blood pressure in these animals. Thus, the antihypertensive effect of ALLO, shown in our study, can be attributed not only to renal UA normalization, but also to reduction of oxidative stress.

Both renal UA and ROS production, which are reduced by ALLO, can activate NLRP3 inflammasome [14, 15], whereas their suppression can inhibit this effect. Accordingly, evidence is growing that ALLO suppresses renal NLRP3 activation, resulting in amelioration of renal injury [12]. Previous work had shown that NLRP3 deletion reduces renal fibrosis and reverses mitochondrial dysfunction in the unilateral ureteral obstruction model [6]. In the present study, ALLO treatment attenuated the activity of the NLRP3 pathway, indicated by reduction of both NLRP3 and active caspase 1, thus normalizing the production of IL-1β. Importantly, ALLO had no effect on the NF-κB system, another innate immunity component. This finding suggests that the antiinflammatory effect of XOD blockade is essentially due to inhibition of the NLRP3 inflammasome, without interference on the NF-κB pathway. This view is reinforced by the observation that the NLRP3 content correlated significantly with TCP, interstitial

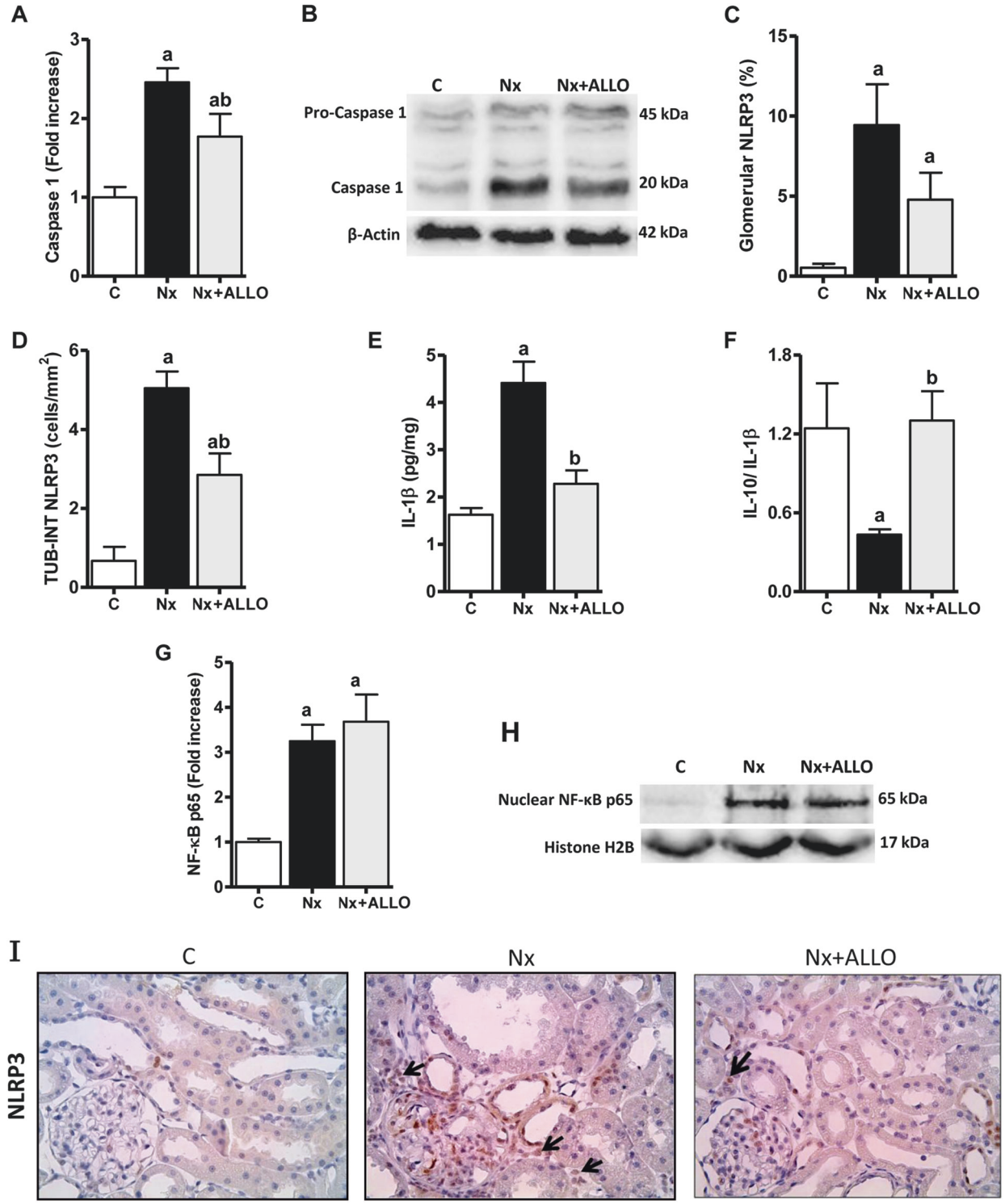

Fig. 4 Renal content of caspase 1 (**a**) was evaluated by western blot analysis (**b**). The presence of NLRP3 (%) in glomeruli (**c**) and the number of NLRP3-positive cells (cells/mm^2) in the tubulointerstitial (TUB-INT) compartment (**d**) were evaluated using immunohistochemistry staining. Protein levels of IL-1β (pg/mL) (**e**) and the IL-10 and IL-1β contents (**f**) were quantified by ELISA. To evaluate the NF-κB activation in renal tissue, the phosphorylated p65 content was quantified in nuclei (**g**) by western blot analysis (**h**). Histone H2B was used as loading control. Illustrative microphotographs show the presence of NLRP3-positive staining in glomeruli, and NLRP3-positive cells in tubules or at the interstitium (arrows) (×400) (**i**). Results expressed as means ± SE. $^{a}p < 0.05$ vs. C, $^{b}p < 0.05$ vs. Nx

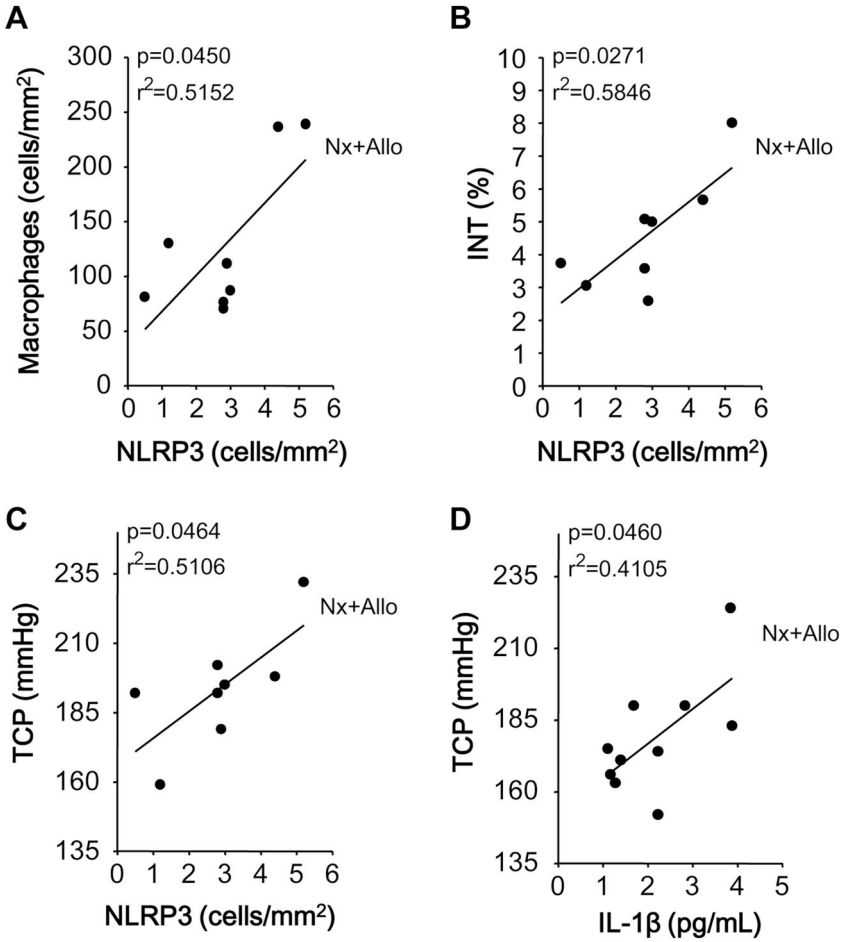

Fig. 5 Correlations (in the Nx + ALLO group) between interstitial macrophage infiltration (cells/mm^2) and tubulointerstitial NLRP3 + cells (cells/mm^2) (**a**), percentage of cortical interstitial area (INT, %) and tubulointerstitial NLRP3 + cells (cells/mm^2) (**b**), tail-cuff pressure (TCP, mmHg) and tubulointerstitial NLRP3 + cells (cells/mm^2) (**c**), and tail-cuff pressure (TCP, mmHg) and renal protein content of IL-1β (pg/mL) (**d**). Correlation analyses were restricted to the animals in which the ELISA or immunohistochemical analyses were performed. Significant correlations were established according to the Pearson's coefficient ($p < 0.05$)

expansion and the density of interstitial macrophage infiltration, whereas the content of IL-1β correlated with TCP.

In summary, our observations indicate that the antiinflammatory and antifibrotic effect of ALLO in the Nx model involves inhibition of the NLRP3, but not of the NF-κB pathway. The fact that ALLO-induced renoprotection was incomplete suggests that the NF-κB system and/or other signaling pathways may also participate in the pathogenesis of renal injury associated with this model. Whatever the mechanisms involved, ALLO may play a role in the quest to arrest or detain the progression of CKD.

Acknowledgements These studies were supported by the São Paulo Research Foundation (FAPESP- grant n° 2011/19576-4, n° 2012/10926-5 and n° 2013/12256-0) and the National Council for Scientific and Technological Development (CNPq) award (303684/2013-5). Moreover, the Authors thank to Claudia R. Sena, Camilla Fanelli, Vivian L. Viana, and Janice G. P. Silva, for expert technical assistance.

Compliance with Ethical Standards

Conflict of interest :The authors declare that they have no conflict of interest.

References

1. Fanelli C, Arias SCA, Machado FG, et al. Innate and adaptive immunity are progressively activated in parallel with renal injury in the 5/6 Renal ablation model. Sci Rep. 2017;7:3192.
2. Vilaysane A, Chun J, Seamone ME, et al. The NLRP3 inflammasome promotes renal inflammation and contributes to CKD. J Am Soc Nephrol. 2010;21:1732–44.
3. Anders HJ, Muruve DA. The inflammasomes in kidney disease. J Am Soc Nephrol. 2011;22:1007–18.
4. Fang L, Xie D, Wu X, Cao H, Su W, Yang J. Involvement of endoplasmic reticulum stress in albuminuria induced inflammasome activation in renal proximal tubular cells. PLoS ONE. 2013;8:e72344.
5. Zhuang Y, Ding G, Zhao M, et al. NLRP3 inflammasome mediates albumin-induced renal tubular injury through impaired mitochondrial function. J Biol Chem. 2014;289:25101–11.
6. Guo H, Bi X, Zhou P, Zhu S, Ding W. NLRP3 deficiency attenuates renal fibrosis and ameliorates mitochondrial dysfunction in a mouse unilateral ureteral obstruction model of chronic kidney disease. Mediat Inflamm. 2017;2017:8316560.
7. Martinon F, Mayor A, Tschopp J. The inflammasomes: guardians of the body. Annu Rev Immunol. 2009;27:229–65.
8. Schroder K, Tschopp J. The inflammasomes. Cell. 2010;140:821–32.
9. Zhou R, Tardivel A, Thorens B, Choi I, Tschopp J. Thioredoxin-interacting protein links oxidative stress to inflammasome activation. Nat Immunol. 2010;11:136–40.

10. Muruve DA, Petrilli V, Zaiss AK, et al. The inflammasome recognizes cytosolic microbial and host DNA and triggers an innate immune response. Nature. 2008;452:103–7.
11. Mariathasan S, Weiss DS, Newton K, et al. Cryopyrin activates the inflammasome in response to toxins and ATP. Nature. 2006;440:228–32.
12. Kim SM, Lee SH, Kim YG, et al. Hyperuricemia-induced NLRP3 activation of macrophages contributes to the progression of diabetic nephropathy. Am J Physiol Ren Physiol. 2015;308: F993–1003.
13. Mulay SR, Anders HJ. Crystal nephropathies: mechanisms of crystal-induced kidney injury. Nat Rev Nephrol. 2017;13:226–40.
14. Braga TT, Forni MF, Correa-Costa M, et al. Soluble uric acid activates the NLRP3 inflammasome. Sci Rep. 2017;7:39884.
15. Nicholas SA, Bubnov VV, Yasinska IM, Sumbayev VV. Involvement of xanthine oxidase and hypoxia-inducible factor 1 in Toll-like receptor 7/8-mediated activation of caspase 1 and interleukin-1beta. Cell Mol Life Sci. 2011;68:151–8.
16. Siu YP, Leung KT, Tong MK, Kwan TH. Use of allopurinol in slowing the progression of renal disease through its ability to lower serum uric acid level. Am J Kidney Dis. 2006;47:51–9.
17. Bakris GL, Lass N, Gaber AO, Jones JD, Burnett JC. Radiocontrast medium-induced declines in renal function: a role for oxygen free radicals. Am J Physiol. 1990;258:F115–20.
18. Correa-Costa M, Braga TT, Semedo P, et al. Pivotal role of Toll-like receptors 2 and 4, its adaptor molecule MyD88, and inflammasome complex in experimental tubule-interstitial nephritis. PLoS ONE. 2011;6:e29004.
19. Goicoechea M, de Vinuesa SG, Verdalles U, et al. Effect of allopurinol in chronic kidney disease progression and cardiovascular risk. Clin J Am Soc Nephrol. 2010;5:1388–93.
20. Kosugi T, Nakayama T, Heinig M, et al. Effect of lowering uric acid on renal disease in the type 2 diabetic db/db mice. Am J Physiol Ren Physiol. 2009;297:F481–8.
21. Bose B, Badve SV, Hiremath SS, et al. Effects of uric acid-lowering therapy on renal outcomes: a systematic review and meta-analysis. Nephrol Dial Transplant. 2014;29:406–13.
22. Arias SC, Valente CP, Machado FG, et al. Regression of albuminuria and hypertension and arrest of severe renal injury by a losartan-hydrochlorothiazide association in a model of very advanced nephropathy. PLoS ONE. 2013;8:e56215.
23. Teles F, Machado FG, Ventura BH, et al. Regression of glomerular injury by losartan in experimental diabetic nephropathy. Kidney Int. 2009;75:72–9.
24. Wallenstein S, Zucker CL, Fleiss JL. Some statistical methods useful in circulation research. Circ Res. 1980;47:1–9.
25. Johnson RJ, Rideout BA. Uric acid and diet--insights into the epidemic of cardiovascular disease. N Engl J Med. 2004;350:1071–3.
26. Truszkowski R, Goldmanówna C. Uricase and its action: distribution in various animals. Biochem J. 1933;27:612–4.
27. Bolisetty S, Zarjou A, Agarwal A. Heme oxygenase 1 as a therapeutic target in acute kidney injury. Am J Kidney Dis. 2017;69:531–45.
28. Becuwe P, Ennen M, Klotz R, Barbieux C, Grandemange S. Manganese superoxide dismutase in breast cancer: from molecular mechanisms of gene regulation to biological and clinical significance. Free Radic Biol Med. 2014;77:139–51.
29. Henkel T, Machleidt T, Alkalay I, Krönke M, Ben-Neriah Y, Baeuerle PA. Rapid proteolysis of I kappa B-alpha is necessary for activation of transcription factor NF-kappa B. Nature. 1993;365:182–5.
30. Anderson S, Rennke HG, Brenner BM. Therapeutic advantage of converting enzyme inhibitors in arresting progressive renal disease associated with systemic hypertension in the rat. J Clin Invest. 1986;77:1993–2000.
31. Lafayette RA, Mayer G, Park SK, Meyer TW. Angiotensin II receptor blockade limits glomerular injury in rats with reduced renal mass. J Clin Invest. 1992;90:766–71.
32. Yang N, Wu LL, Nikolic-Paterson DJ, et al. Local macrophage and myofibroblast proliferation in progressive renal injury in the rat remnant kidney. Nephrol Dial Transplant. 1998;13:1967–74.
33. Fujihara CK, Malheiros DM, Zatz R, Noronha IL. Mycophenolate mofetil attenuates renal injury in the rat remnant kidney. Kidney Int. 1998;54:1510–9.
34. Kliem V, Johnson RJ, Alpers CE, et al. Mechanisms involved in the pathogenesis of tubulointerstitial fibrosis in 5/6-nephrectomized rats. Kidney Int. 1996;49:666–78.
35. Fujihara CK, Antunes GR, Mattar AL, Malheiros DM, Vieira JM, Zatz R. Chronic inhibition of nuclear factor-kappaB attenuates renal injury in the 5/6 renal ablation model. Am J Physiol Ren Physiol. 2007;292:F92–9.
36. Schreck R, Rieber P, Baeuerle PA. Reactive oxygen intermediates as apparently widely used messengers in the activation of the NF-kappa B transcription factor and HIV-1. EMBO J. 1991;10:2247–58.
37. Fridovich I. Superoxide dismutases. An adaptation to a paramagnetic gas. J Biol Chem. 1989;264:7761–4.
38. Sánchez-Lozada LG, Tapia E, Santamaría J, et al. Mild hyperuricemia induces vasoconstriction and maintains glomerular hypertension in normal and remnant kidney rats. Kidney Int. 2005;67:237–47.
39. Feig DI, Soletsky B, Johnson RJ. Effect of allopurinol on blood pressure of adolescents with newly diagnosed essential hypertension: a randomized trial. JAMA. 2008;300:924–32.
40. Kanbay M, Ozkara A, Selcoki Y, et al. Effect of treatment of hyperuricemia with allopurinol on blood pressure, creatinine clearence, and proteinuria in patients with normal renal functions. Int Urol Nephrol. 2007;39:1227–33.
41. Riegersperger M, Covic A, Goldsmith D. Allopurinol, uric acid, and oxidative stress in cardiorenal disease. Int Urol Nephrol. 2011;43:441–9.
42. Dummer CD, Thomé FS, Veronese FV. [Chronic renal disease, inflammation and atherosclerosis: new concepts about an old problem]. Rev Assoc Med Bras. 1992;2007:446–50.
43. Nakazono K, Watanabe N, Matsuno K, Sasaki J, Sato T, Inoue M. Does superoxide underlie the pathogenesis of hypertension? Proc Natl Acad Sci USA. 1991;88:10045–8.